Proceedings of ASME Turbo Expo 2011
GT2011
June 6-10, 2011, Vancouver, British Columbia, Canada

GT2011-45428

FILM COOLING EFFECTIVENESS DISTRIBUTION ON FIRST-STAGE VANE ENDWALL WITH AND WITHOUT LEADING-EDGE FILLETS PART II：EFFECT OF INCIDENCE ANGLE

Yang Zhang, Xin Yuan
Key Laboratory for Thermal Science and Power Engineering of Ministry of Education
Tsinghua University
Beijing 100084, P.R. China
Email: zhangyange436@yahoo.com.cn

ABSTRACT

Using the leading edge airfoil fillet to reduce the aerodynamic loss and surface heat transfer has been proved effective, while the factor of film cooling has not been considered. The first part of the research indicates that the leading edge fillet could improve the film cooling effectiveness through controlling the secondary flow, while this conclusion is restricted to the design condition. The flow field at off-design condition is different from that of the design condition, especially for the structure of horseshoe vortex at the leading edge. It's possible that the advantage of fillets is not reliable at positive or negative inlet flow angle conditions, which makes the investigation on endwall film cooling with leading edge modification at off-design condition necessary. This paper, which is the second part of a two-part series research investigating the effects of leading edge modification on endwall film cooling, is focused on the performance of fillets at off-design condition. The influence of incidence angle on film cooling effectiveness is studied on first-stage vane endwall with and without leading-edge fillets. A baseline configuration and three kinds of leading edge airfoil fillets are tested in a low speed four-blade cascade consisting of large scale model of the GE-E^3 Nozzle Guide Vane (NGV). The results show that as the incidence angle varies from i=+10 deg to i=−10 deg, at low blowing ratio the film cooling effectiveness decreases near the leading edge suction side for all the leading edge geometries. However, this trend becomes opposite under high blowing ratio that the lowest film cooling effectiveness condition is at the incidence angle of i=+10 deg. Near the leading edge pressure side, the film cooling effectiveness increases as the incidence angle varies from i=+10 deg to i= −10 deg at all blowing ratios in the research. The change of incidence angle causes the peak of laterally averaged effectiveness in this region to shift upstream. The experimental results also indicate that the longfillet has the lowest sensitivity towards incidence angle. As for the main passage endwall, with the incidence angle changing form i=+10 deg to i=-10 deg the averaged film cooling effectiveness increases, while this trend will be eliminated by increasing the blowing ratio.

INTRODUCTION

Higher performance of future gas turbines desires an improvement of efficiencies which is usually achieved by increasing the turbine inlet temperatures. However, the turbine inlet temperatures (about 1600 ºC) are generally above the material failure limit of turbine components (about 1300 ºC), which drives the need for newer cooling methods that reduce thermal loads on the turbine components. Methods such as film cooling and internal cooling have led to improvements in modern gas turbine performance.

As for the blade platform film cooling research, Yang and Gao et al. [1] used numerical simulation to predict the film cooling effectiveness and heat transfer coefficient distributions on a rotating blade platform with stator-rotor purge flow and downstream discrete film-hole flows in a 1-1/2 turbine stage. The effect of turbine work process on the film cooling effectiveness and the associated heat transfer coefficients had been reported. [1] Wright et al. [2] used the PSP (pressure sensitive paint) technique to measure the film cooling effectiveness on a turbine blade platform due to three different stator-rotor seals. Three slot configurations placed upstream of the blades were used to model advanced seals between the stator and rotor. PSP was proven to be a valuable tool to obtain detailed film cooling effectiveness distributions. Gao et al. [3] studied turbine blade platform film cooling with typical stator-rotor purge flow and discrete-hole film cooling. The shaped holes presented higher film-cooling effectiveness and wider film coverage than the cylindrical holes, particularly at higher blowing ratios. The detailed film cooling effectiveness distributions on the platform were also obtained using PSP technique. Results showed that the combined cooling scheme (slot purge flow cooling combined with discrete-hole film cooling) was able to provide full film coverage on the platform. [3] The measurements were obtained by Charbonnier et al. [4] applying the PSP technique to measure the coolant gas concentration. An engine representative density ratio between the coolant and the external hot gas flow was achieved by the injection of CO_2. [4] Zhang et al. [5] used the back-facing step to simulate the discontinuity of the nozzle inlet to the combustor exit cone. Nitrogen gas was used to simulate cooling flow as well as a tracer gas to indicate oxygen concentration such that film effectiveness by the mass transfer analogy could be obtained. [5]

The effects of leading edge modification on endwall heat transfer have been investigated by many researchers. Saha et al. [6] studied the role of leading-edge contouring on endwall flow and heat transfer. Numerical predictions and measurements of the flow structure and the Nusselt number behavior were presented for the endwall region of a linear blade cascade with contoured leading edge fillets. The pitchwise

pressure gradient and shear stress on the endwall region were reduced for the filleted blades compared to the baseline case where there was no fillet. [6] Mahmood et al. [7] measured endwall flow and passage heat transfer in a linear blade passage with endwall and leading edge modifications. The results indicated that the leading edge fillets could not significantly influence the blade surface pressure distributions near the endwall. However, the weaker and smaller passage vortex for the contour endwall and fillets could reduce the endwall heat transfer and the Nusselt numbers along the endwall especially upstream of the mid-passage location. [7] Barberis and Molton et al. [8] used an active control system, with suction through a hole located in the plane of symmetry in front of the obstacle's leading edge, where the vortex size was reduced and its location displaced towards the origin of the obstacle. [8] Paik et al. [9] studied the bimodal dynamics of the turbulent horseshoe vortex system in a wing-body junction demonstrating the potential of DES as a powerful simulation tool for predicting complex, high Reynolds number flows dominated by organized coherent structures. [9] Gregory-Smith et al. [10] found the effect of leading edge extension could reduce the secondary flow by unloading the leading edge of the blade. [10] Green et al. [11] developed a design method whereby the flow separation in the wing-fuselage juncture of aircraft is eliminated by the use of a leading-edge fillet. Using the design rule, the skin friction distribution is moved toward the target distribution by extending the leading edge of the wing to form a leading-edge fillet.[11]

The studies of incidence angle effect on flow field and heat transfer were also preformed by researchers. A series of AIAA papers were focused on the function of leading edge fillet at different incidence angles. The results showed that with the appendage at zero angle of attack, the fillet eliminated leading-edge separation and thus the formation of a horseshoe vortex around the wing nose. It greatly improved the stability of the flow close to the junction and the nonuniformity of its wake. At nonzero angles of attack, the desirable effects of the fillet were reduced apparently because of separation of the body boundary layer as it approached the pressure side of the fillet.[12][13][14] Gao et al. [15] studied the influence of incidence angle on film cooling effectiveness for a cutback squealer blade tip. Three incidence angles were investigated 0 deg at design condition and ±5 deg at off-design conditions. Based on mass transfer analogy, the film-cooling effectiveness is measured with PSP techniques. It was observed that the incidence angle affected the coolant jet direction on the pressure side near tip region and the blade tip. The film-cooling effectiveness distribution was also altered. [15] Montomoli et al. [16] studied the effect of wake passing on a film cooled leading edge with different incidence and injection angles. The separated region near leading edge changed its extension when the incidence angle is different. In particular, the separation interested an higher region of pressure side at negative incidence. [16] Lee et al. [17] studied the effects of incidence angle on the endwall convective transport within a high-turning turbine rotor passage. Surface flow visualizations and heat/mass transfer measurements at off-design conditions were carried out at a fixed inlet Reynolds number for the incidence angles of -10deg, -5 deg, 0 deg, +5 deg, and +10 deg. The results showed that the incidence angle had considerable influences on the endwall local transport phenomena and on the behaviors of various endwall vortices. In the negative incidence case, convective transport was less influenced by the leading edge horseshoe vortex. In the case of positive incidence, however, convective transport was augmented remarkably along the leading edge horseshoe vortex, and is much influenced by the suction-side corner vortex. [17] Benabed et al. [18] numerically investigated the influence of incidence angle on asymmetrical turbine blade model showerhead film cooling effectiveness. The results indicated that variation of operating incidence angle from that fixed by design conditions could strongly affect the thermal protection of the blade especially for the low blowing ratios. The stagnation point moved from the suction side to the pressure side as the incidence angle changing from the negative values to the positive ones. For the lowest value of the incidence angle, the trajectory path of the suction side injection is inversed when the blowing ratio increased, dangerously exposing the suction side to hot gases. [18] Duikeren et al. [19] studied the over-tip casing heat transfer at off-design condition. At part load conditions, the fluid might hit the front section of the suction side of the blade resulting in increased turbulence and heat transfer levels. In severe cases, the boundary layer flowed around the leading edge will separate, which improved the heat transfer even more. [19] Wagner et al. [20] investigated the performance of different film cooling hole configurations at designed and off-designed mainstream incidence angles. At +5deg incidence on the pressure side, a beneficial interaction between the jets of the pressure side row appeared. For middle and high blowing ratio, the film cooling performances were also better than 0deg incidence. [20]

Past research has shown that incidence angles can result in changes to the local heat transfer on the leading edge region. Many studies have investigated the effects of inlet flow angle on the blade showerhead film cooling, indicating the off-design condition could apparently change the injection flow trace. Few studies, however, have considered the combining effect of leading edge fillets and incidence angle on endwall film cooling. To help fill this gap, the current paper discusses the effect of incidence angle on the film cooling of a nozzle guide vane endwall. The effect of varying the fillet geometry and the blowing ratio are also considered. This paper is the second part of a two-part study that also investigates the effect of leading edge geometry on the cooling performance of a film cooled endwall with and without leading edge fillets(PART I).

FILM COOLING EFFECTIVENESS MEASUREMENT THEORY AND DATA ANALYSIS

The film cooling effectiveness was measured using the PSP technique. PSP is a photo luminescent material that excited by visible light at 450 nm, emitting light that could be detected by a high spectral sensitivity CCD camera fitted with a 600 nm band pass filter. The light intensity is inversely proportional to the local partial pressure of oxygen. The layout of the optical system is shown in Fig.1. The image intensity obtained from PSP by the camera is normalized with a reference image intensity (I_{ref}) taken without main stream flow. Background noise in the optical setup is eliminated by subtracting the nitrogen/air injection image intensities with the image intensity obtained without main stream flow and light excitation (I_{blk}). The recorded light intensity ratio can be converted to partial pressure ratio of oxygen with the parameters obtained in calibration, as shown in Eq.(1):

$$\frac{I_{ref}-I_{blk}}{I-I_{blk}} = f\left[\frac{\left(P_{O_2}\right)_{air}}{\left(P_{O_2}\right)_{ref}}\right] = f\left(P_{ratio}\right) \quad (1)$$

Where I represents the intensity obtained at each pixel and $f\left(P_{ratio}\right)$ is the parameter indicating the relationship between intensity ratio and pressure ratio. The film cooling effectiveness can be determined by the correlation between the PSP emitting intensity and the oxygen partial pressure. Calibration of the PSP was performed in a vacuum chamber by varying the pressure from 0 atm to 1.0 atm at three different temperatures, as shown in Fig.2. A PSP coated test coupon was placed in the vacuum chamber with transparent windows through which the camera can detect the light intensity on the coupon surface. The

calibration curve is shown in Fig.3. A temperature difference less than 0.5k between main stream and secondary flow should be guaranteed during the tests. To obtain film cooling effectiveness, both of air and nitrogen are used as coolant. The molecular weight of nitrogen is nearly the same as that of air, which makes the change in local oxygen partial pressure at a fixed blowing ratio possible. By comparing the difference in oxygen partial pressure between the air and nitrogen injection cases, the film cooling effectiveness can be obtained using the Eq.(2):

$$\eta = \frac{C_{air} - C_{mix}}{C_{air}} = \frac{\left(P_{O_2}\right)_{air} - \left(P_{O_2}\right)_{mix}}{\left(P_{O_2}\right)_{air}} \quad (2)$$

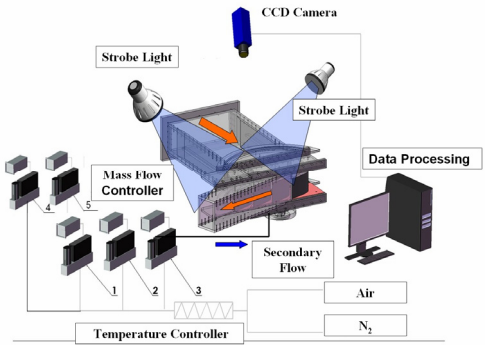

Figure 1. SCHEMATIC OF CASCADE TEST RIG.

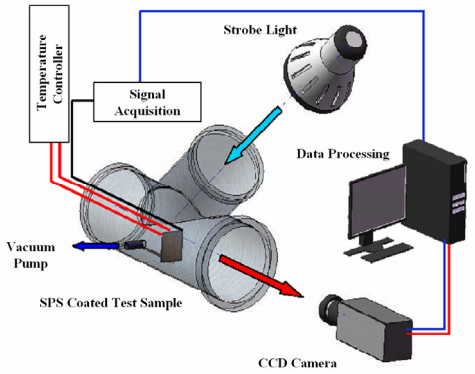

Figure 2. CALIBRATION SYSTEM.

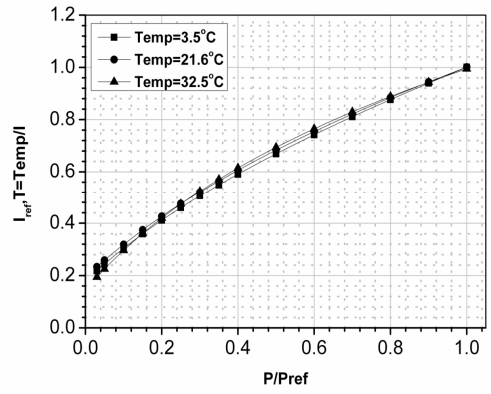

Figure 3. CALIBRATION CURVE FOR PSP.

EXPERIMENTAL FACILITY

As shown in Fig.4, the test section consists of an inlet duct, a linear turbine cascade, and an exhaust section. The inlet duct has a cross section of 318 mm (width) and 129 mm (height).To study different mainstream inlet angles, the guide vanes are placed on a rotatable half-circular plate, which serves as part of the endwall, as shown in Fig.4. By turning the half-circular plate, incidence angles at design and off-design conditions are achieved. During the test, the tail boards, and the CCD camera were moved with the rotatable plate to the same relative position as that at incidence angle of 0deg. In this study, three different positions were chosen for the incidence angles of i = -10 deg, 0deg and +10 deg. During the test, the cascade inlet air velocity was maintained at 35 m/s for all the inlet flow conditions, which corresponds to a Mach number of 0.1. A two times scaled model of the GE-E^3 guide vanes with a blade span of 129 mm and an axial chord length of 72.5 mm was used.

Four rows of compound angle laidback fan-shaped holes are arranged on the endwall to form full covered coolant film. Fig.5 shows the holes configurations and the blade geometric parameters. The first row is located upstream of the leading edge plane. The following three rows are evenly positioned inside the vane channel, with the last one located at 65% axial chord downstream of the leading edge plane. The four rows of fanshaped holes are inclined 30 deg to the platform surface and held an angle of 0, 30, 45 and 60 deg to axial direction respectively. The laidback fanshaped holes are featured with a lateral expansion of 10 deg from the hole-axis and forward expansion of 10 deg into the endwall surface, as shown in Fig.6. The diameter in metering part (cylindrical part) of the shaped holes is 1.2 mm, and the expansion starts at 4.2D. Four coolant cavities are used for the four rows of holes respectively, as shown in Fig.6 (The extra coolant plenum chamber is designed to simulate the purge flow which is not used in this experiment). The coolant supplied to each cavity is independently controlled by a rotameter dedicated to that cavity. Three types of fillets were investigated in the experiment. As shown in Fig.7, the longfillet is 18.8 mm long, 9.48 mm high, resulting in an aspect ratio of 0.5. The geometric parameters of the other two types of fillets are also shown in Fig.7. The uncertainties of the dimensionless temperature and the film cooling effectiveness are estimated as 3% at a typical value of 0.5 based on 95% confidence interval. When the value is approaching zero, the uncertainty rises. For instance, the uncertainty is approximately 8% at the value of 0.05.

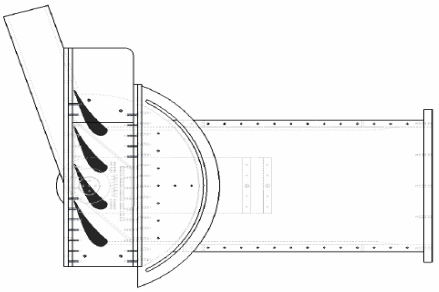

Figure 4. SCHEMATIC OF THE TEST SECTION WITH ROTATABLE CASCADE

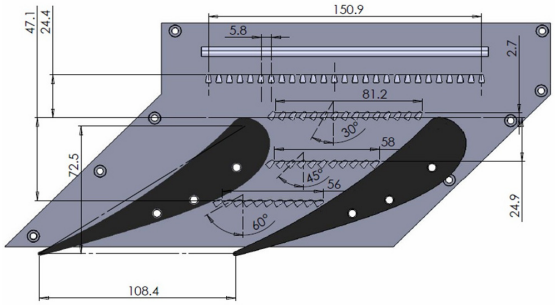

Figure 5. FILM COOLING HOLE CONFIGURATION ON ENDWALL.

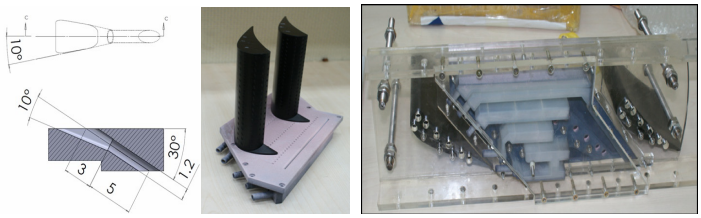

Figure 6. COOLANT SUPPLY CAVITIES, LAIDBACK FAN-SHAPED HOLE, VANES WITH FILLET.

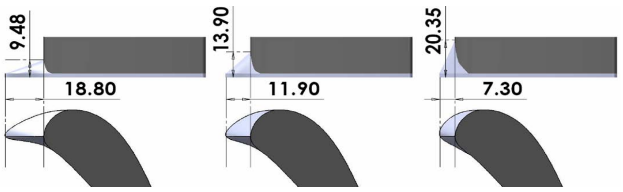

Figure 7. LONG, MEDIUM AND SHORT FILLET GEOMETRIES.

RESULTS AND DISCUSSION

As discussed in the first part of this research which is focused on the effect of leading edge geometry, the region along pressure side near leading edge is necessary to be investigated in detail. A narrow region along leading edge pressure side is selected (blue lines near the pressure side), as shown in Fig.8-10, where the film cooling effectiveness distributions at different incidence angles are compared. For the baseline case (Fig.8-10), at low blowing ratio condition (M=0.4, Fig.8), the injection flow traces near the leading edge could not enter the region investigated at any incidence angle in this research, indicating that with low momentum the injection flow could not overcome the influence of horseshoe vortex at design and off-design condition. The same phenomenon could be found in the shortfillet case (Fig.13) and mediumfillet case (Fig.18). When the blowing ratio increases to M=0.8 (Fig.9), the cooling flow traces could reach the surface of leading edge pressure side. The length of the coolant trace decreases with de incidence angle changing from i=-10 deg to i=+10 deg, which shows that the positive incidence angle would force the coolant flow to move towards pressure side, resulting in a lower film cooling effectiveness in the region investigated. The same phenomenon could be found for the blowing ratio of M=1.2 (Fig.10). The different injection flow behavior at the blowing ratio of M=0.8 in shortfillet case (Fig.14) and mediumfillet case (Fig.19) could be compared with that of the nofillet case (Fig.9). For the baseline case, this blowing ratio is strong enough for the coolant to enter the region near pressure side, but for the shortfillet case and mediumfillet case this phenomenon does not occur. The coolant flow trace is kept out of the near pressure side region, leaving an uncooled area. When the blowing ratio increases to M=1.2, the coolant has enough momentum to enter the near pressure side region, as shown in Fig.15 and Fig.20.

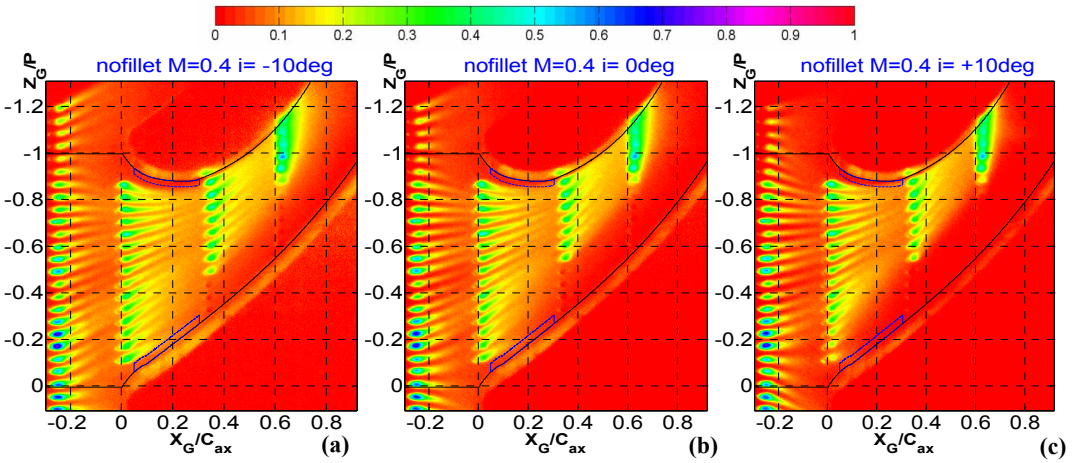

Figure 8. FILM COOLING EFFECTIVENESS DISTRIBUTION ON THE ENDWALL AT DIFFERENT INCIDENCE ANGLE.

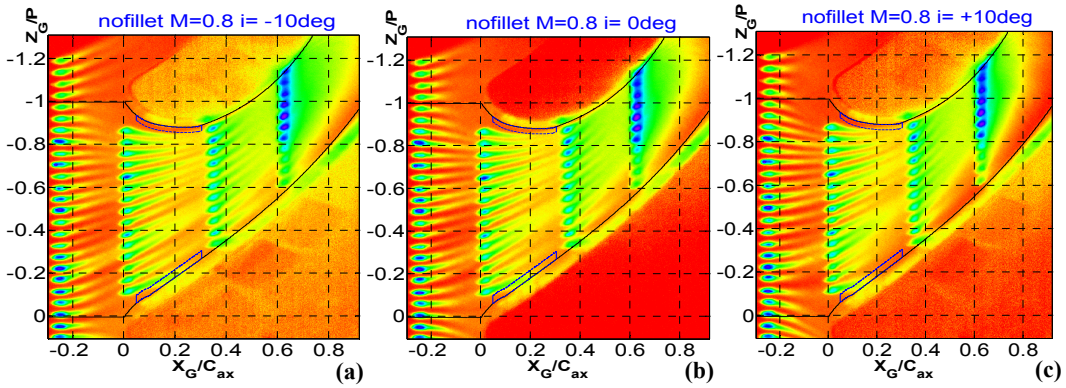

Figure 9. FILM COOLING EFFECTIVENESS DISTRIBUTION ON THE ENDWALL AT DIFFERENT INCIDENCE ANGLE.

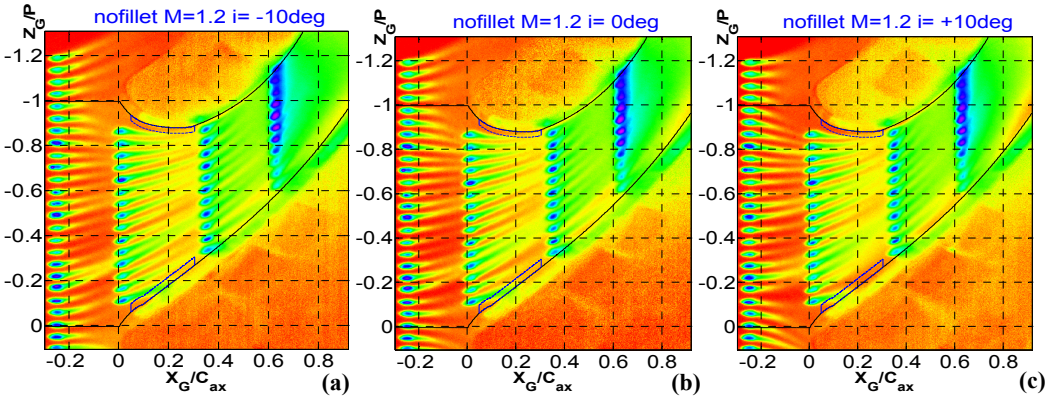

Figure 10. FILM COOLING EFFECTIVENESS DISTRIBUTION ON THE ENDWALL AT DIFFERENT INCIDENCE ANGLE.

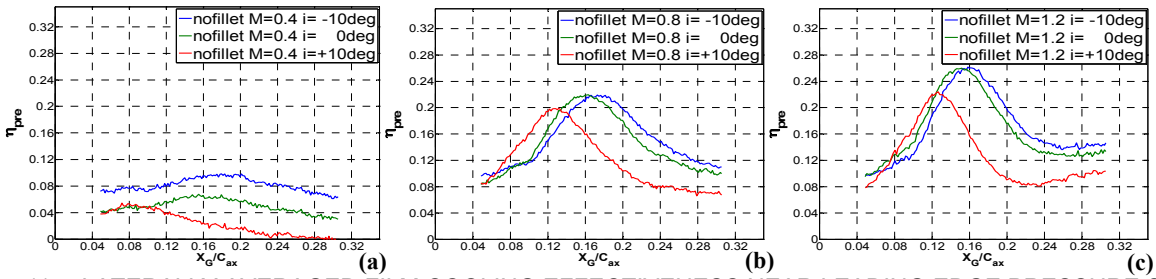

Figure 11. LATERALLY AVERAGED FILM COOLING EFFECTIVENESS NEAR LEADING EDGE PRESSURE SIDE.

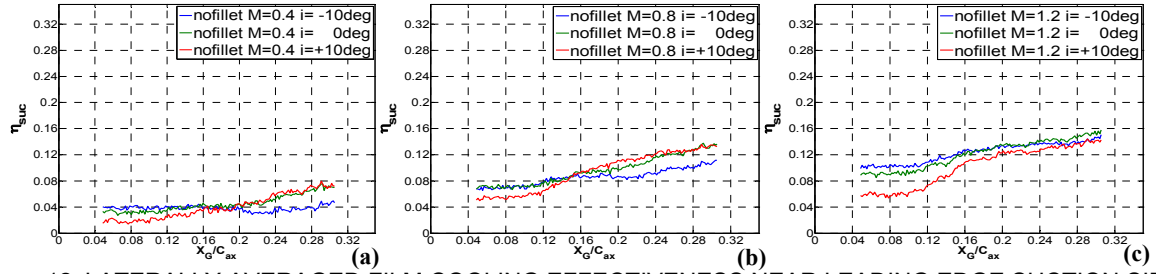

Figure 12. LATERALLY AVERAGED FILM COOLING EFFECTIVENESS NEAR LEADING EDGE SUCTION SIDE.

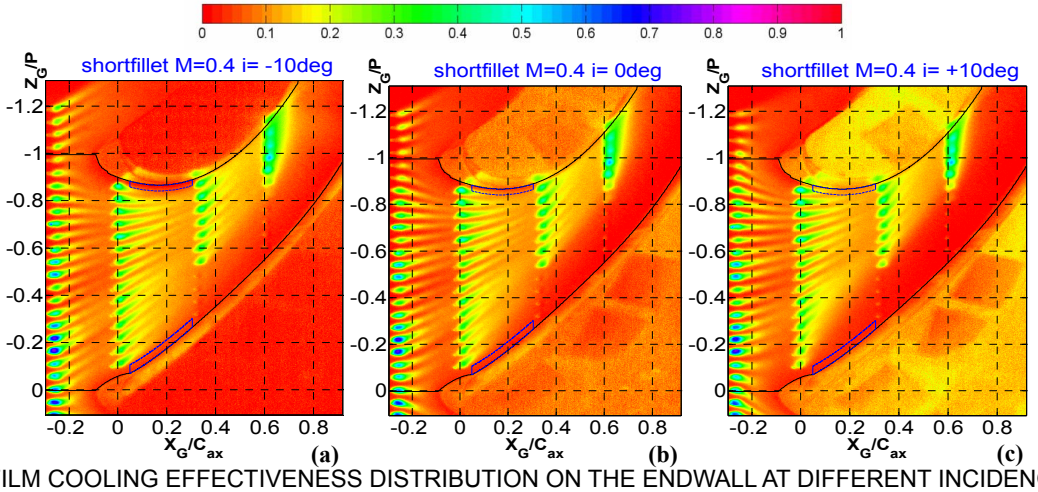

Figure 13. FILM COOLING EFFECTIVENESS DISTRIBUTION ON THE ENDWALL AT DIFFERENT INCIDENCE ANGLE.

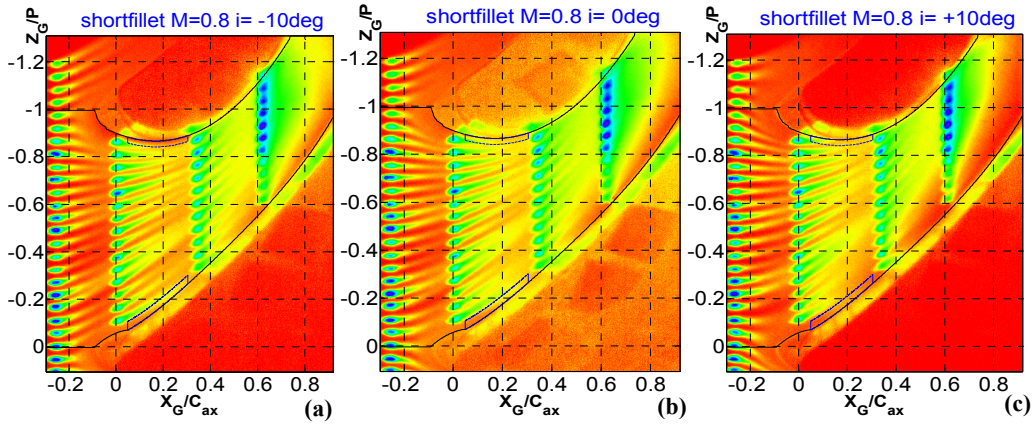

Figure 14. FILM COOLING EFFECTIVENESS DISTRIBUTION ON THE ENDWALL AT DIFFERENT INCIDENCE ANGLE.

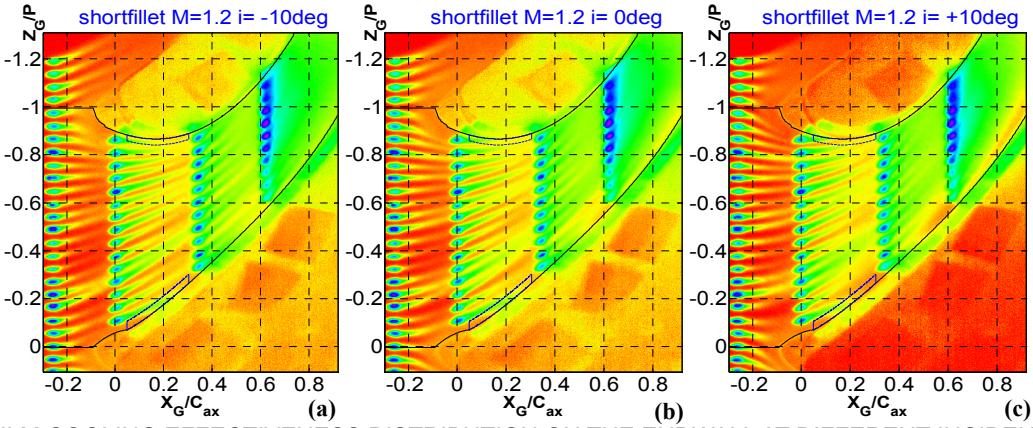

Figure 15. FILM COOLING EFFECTIVENESS DISTRIBUTION ON THE ENDWALL AT DIFFERENT INCIDENCE ANGLE.

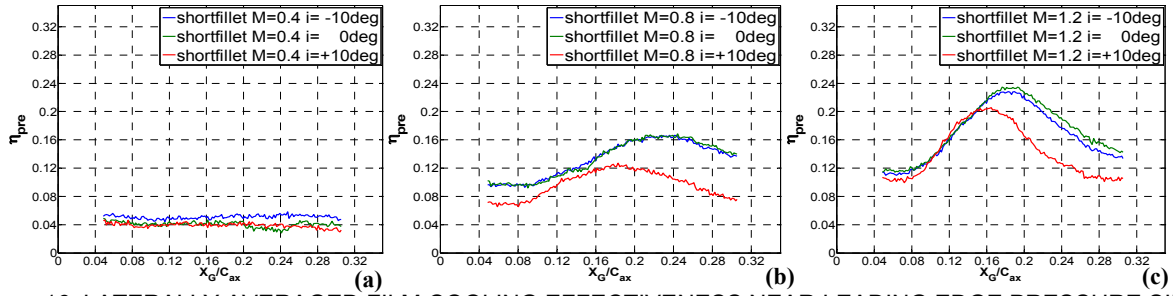

Figure 16. LATERALLY AVERAGED FILM COOLING EFFECTIVENESS NEAR LEADING EDGE PRESSURE SIDE.

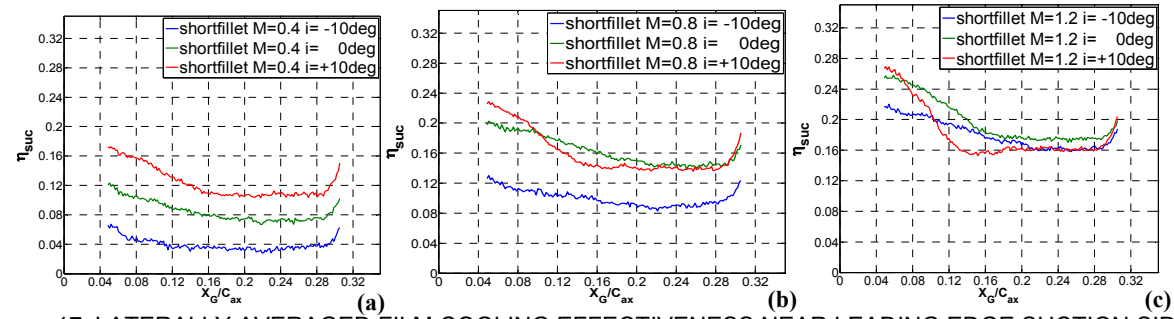

Figure 17. LATERALLY AVERAGED FILM COOLING EFFECTIVENESS NEAR LEADING EDGE SUCTION SIDE.

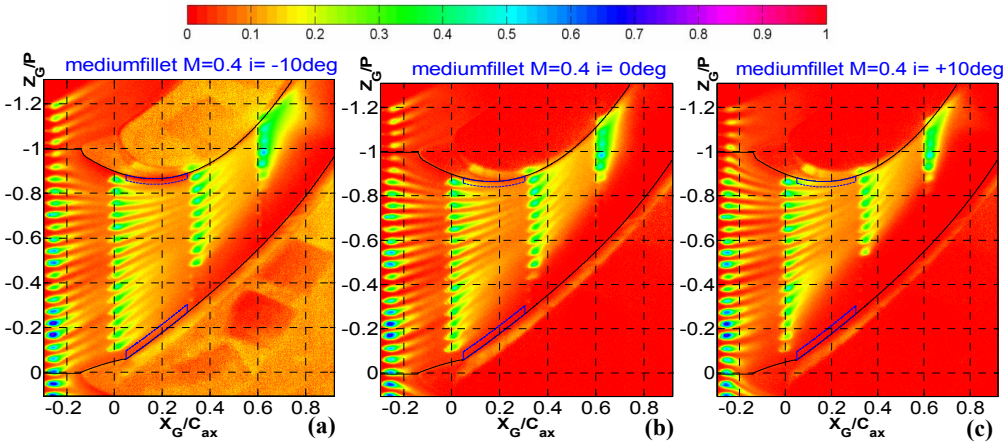

Figure 18. FILM COOLING EFFECTIVENESS DISTRIBUTION ON THE ENDWALL AT DIFFERENT INCIDENCE ANGLE.

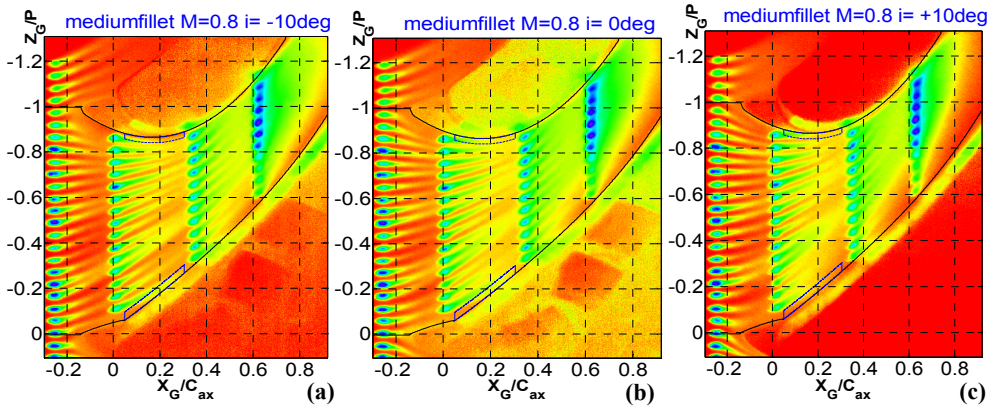

Figure 19. FILM COOLING EFFECTIVENESS DISTRIBUTION ON THE ENDWALL AT DIFFERENT INCIDENCE ANGLE.

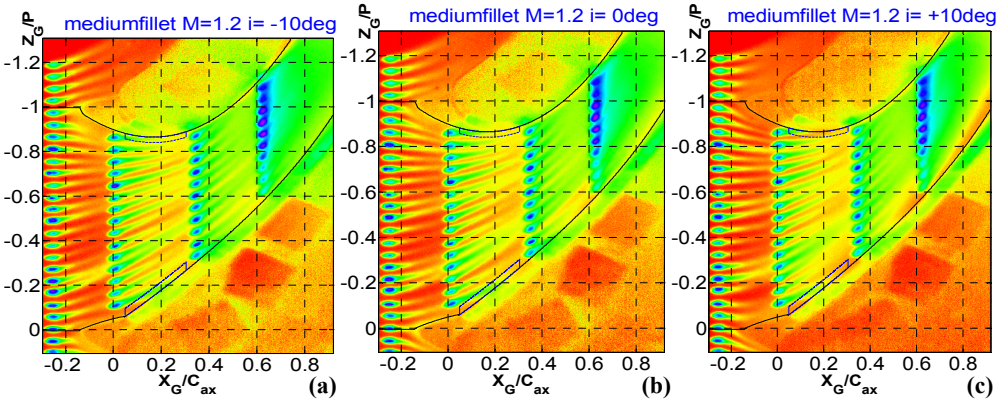

Figure 20. FILM COOLING EFFECTIVENESS DISTRIBUTION ON THE ENDWALL AT DIFFERENT INCIDENCE ANGLE.

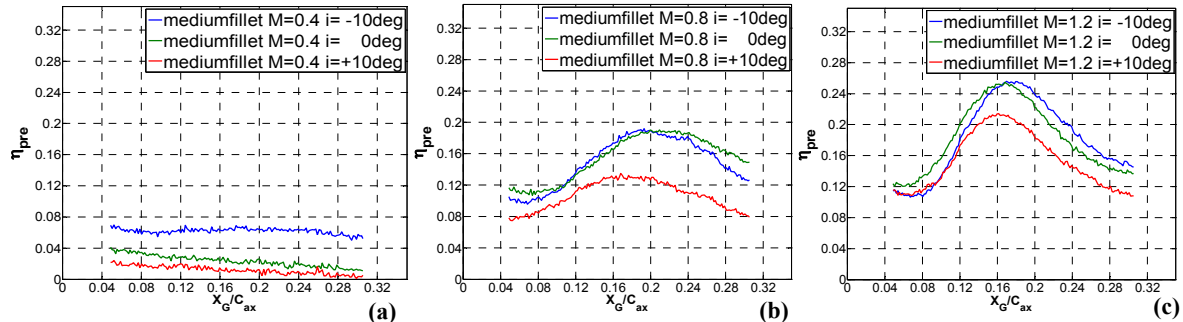

Figure 21. LATERALLY AVERAGED FILM COOLING EFFECTIVENESS NEAR LEADING EDGE PRESSURE SIDE.

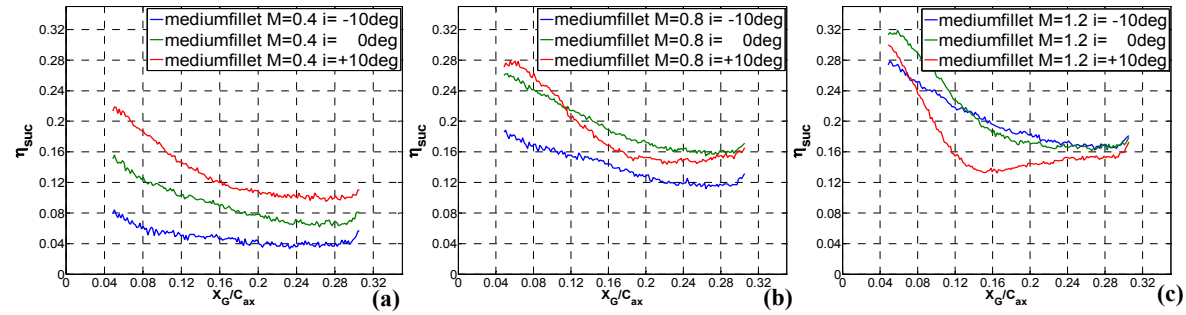

Figure 22. LATERALLY AVERAGED FILM COOLING EFFECTIVENESS NEAR LEADING EDGE SUCTION SIDE.

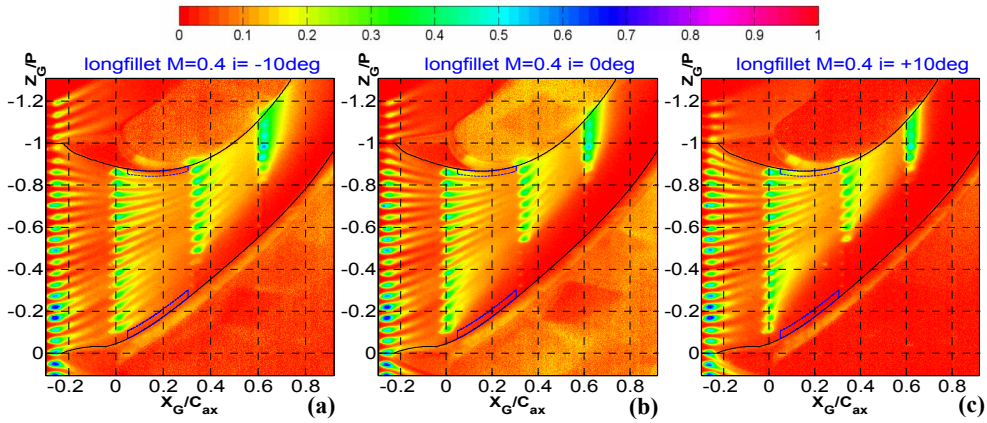

Figure 23. FILM COOLING EFFECTIVENESS DISTRIBUTION ON THE ENDWALL AT DIFFERENT INCIDENCE ANGLE.

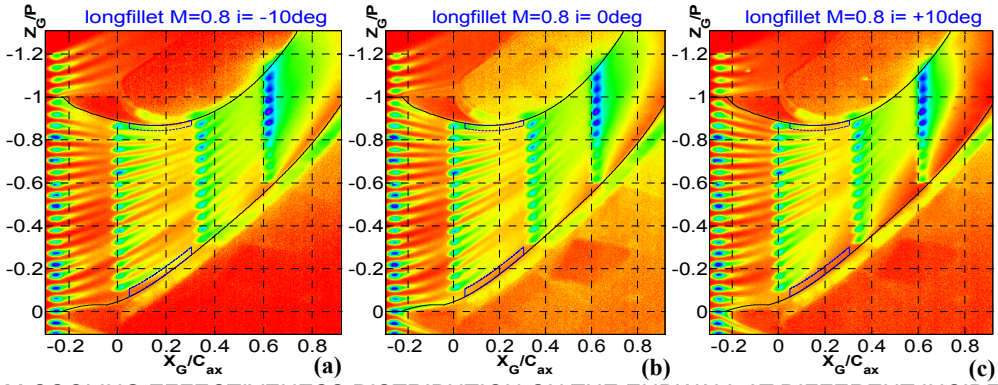

Figure 24. FILM COOLING EFFECTIVENESS DISTRIBUTION ON THE ENDWALL AT DIFFERENT INCIDENCE ANGLE.

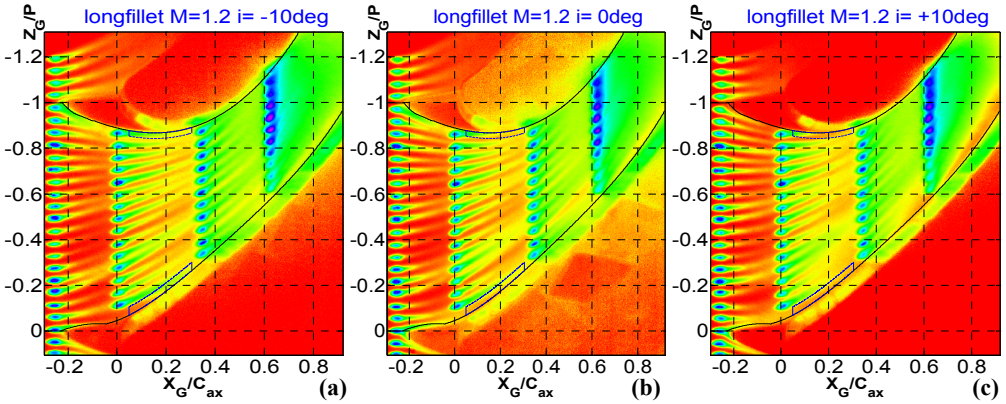

Figure 25. FILM COOLING EFFECTIVENESS DISTRIBUTION ON THE ENDWALL AT DIFFERENT INCIDENCE ANGLE.

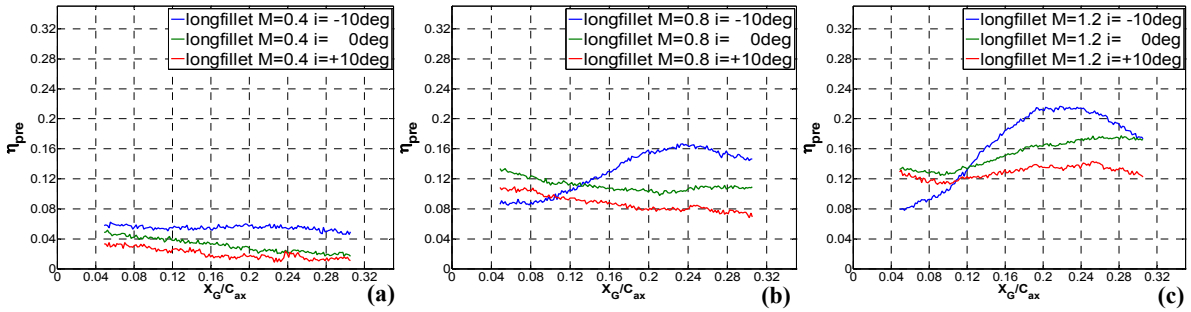

Figure 26. LATERALLY AVERAGED FILM COOLING EFFECTIVENESS NEAR LEADING EDGE PRESSURE SIDE.

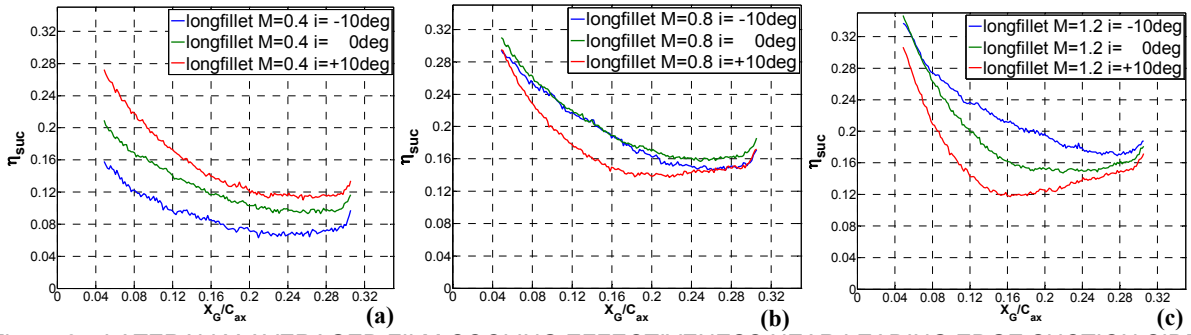

Figure 27. LATERALLY AVERAGED FILM COOLING EFFECTIVENESS NEAR LEADING EDGE SUCTION SIDE.

As shown in Fig.23-25, in the longfillet case, the coolant trace could not enter the narrow region at any incidence angle in the research when the blowing ratio is M=0.4 (Fig.23) and M=0.8 (Fig.24). When the blowing ratio is M=1.2 (Fig.25), the negative incidence angle help the injection flow trace reach the pressure side surface, while the uncooled area is still large at the incidence angle of i=0 deg and i=+10 deg. It indicates that the longer fillet, as well as the positive incidence angle would decrease the film cooling effectiveness near leading edge pressure side. The fillet length and the incidence angle could change the position and strength of horseshoe vortex pressure side leg. A long fillet will make the horseshoe vortex develop earlier before it enters the main passage, which results in a large area along pressure side uncooled. The incidence angle will change the movement direction of horseshoe vortex pressure side leg, forcing the horseshoe vortex to move towards suction side early. This could explain why for every geometry case, the film cooling effectiveness at i=+10 deg is lower than that of i=-10 deg in this region.

Fig.11, Fig.16, Fig.21 and Fig.26 show the laterally averaged film cooling effectiveness along axial chord direction near leading edge pressure side. The computing area could be found in Fig.8-10 (narrow region in blue lines near pressure side). When the blowing ratio is M=0.4 (Fig.11(a), Fig.16(a), Fig.21(d), Fig.26(a)), the film cooling effectiveness distribution is uniform at each incidence angle. For all the leading edge geometries, the leading edge pressure side is protected better at the incidence angle of i=-10 deg, as the film cooling effectiveness is low at the incidence angle of i=+10 deg. Another significant result is that the differences among the three curves representing different incidence angle in baseline case are more apparent than that of the cases with leading edge fillets, which indicates that the fillet is not as sensitive as baseline leading edge to the change of incidence angle. As the blowing ratio increasing to M=0.8 (Fig.11(b), Fig.16(b), Fig.21(b), Fig.26(b)), the filmcooling effectiveness distribution along leading edge pressure side is not uniform as that of low blowing ratio condition.

The peak points in the curves represent the position of coolant traces entering the region investigated, which could be seen in the maps of film cooling effectiveness distribution. The curves in the subplot (b) of Fig.11 shows that in the nofillet case, the coolant flow traces could reach the leading edge pressure side and result in a peak point in film cooling effectiveness curve when the blowing ratio is M=0.8. But the peak points do not occur along the curves in the figures representing fillets cases (Fig.16(b), Fig.21(b), Fig.26(b)) though the curves are not as flat as those in low blowing ratio condition. This indicates that the horseshoe vortex pressure side leg could still strongly dominate this region where the momentum of coolant flow is not big enough for the injection flow to overcome the vortex near the fillets. When the blowing ratio is M=1.2 (Fig.16(c), Fig.21(c)), the injection flow has enough momentum to enter the near pressure side region forming a peak point along the film cooling effectiveness curves, except for the longfillet case (Fig.26(c)) in which the horseshoe vortex pressure side leg develops earlier. The pressure side leg of the horseshoe vortex in the longfillet case develops at the beginning of the fillet which is relatively far from the baseline airfoil leading edge. Then the vortex has enough space to fatherly develop into a strong one providing the force preventing the coolant trace moving towards the longfillet pressure side. This is the reason why no peak points could be found in Fig.26(c).

Fig.8-10 also show the film cooling effectiveness distributions along the leading edge suction side at different incidence angles for the baseline case. Each group of contours compares the distributions of film cooling effectiveness at a fixed blowing ratio. As shown in Fig.8, at low blowing ratio of M=0.4, the injection flow traces could not enter the region (blue lines leading edge suction side) while the uncooled area becomes smaller with incidence angle changing from i=-10 deg to i=+10 deg. It's an opposite trend from that near pressure side. The phenomenon could also be found by comparing the uncooled area near suction side at higher blowing ratio M=0.8 (Fig.9) and M=1.2 (Fig.10). As shown in Fig.9 and Fig.10, with the blowing ratio increasing, the injection flow traces could reach the rear part of leading edge suction side, especially at the incidence angle of i=+10 deg. The positive incidence angle would force the stagnation point to move towards pressure side, which leads the core of horseshoe vortex suction side leg to move towards pressure side. This movement of the horseshoe vortex suction side leg results in a smaller uncooled area in the region investigated. For shortfillet and mediumfillet cases shown in Fig.13-15 and Fig.18-20 apparent uncooled area near leading edge suction side could be found at low blowing ratio M=0.4 (Fig.13, Fig.18), while this area becomes smaller with the blowing ratio increasing to M=0.8

(Fig.14, Fig.19) and M=1.2 (Fig.15,Fig.20). A different trend from that of baseline could be found at higher blowing ratio. With the incidence angle changing from i=-10deg to i=+10deg, the cooled area in the region does not increase continuously. When the blowing ratio is M=0.8, at incidence angle of i=-10 deg (Fig.14(a), Fig.19(a)) uncooled area could be seen, and then this area becomes smaller with the incidence angle changing to i=0 deg and i=+10 deg. However, the length of the injection trace near suction side at the incidence angle of i=+10 deg (Fig.14(c), Fig.19(c)) is shorter than that of i=0 deg condition (Fig.14(b), Fig.19(b)), indicating that the injection flow hit the suction side directly rather than flow downstream. The short injection flow trace at positive incidence angle could be apparently seen in the longfillet case (Fg.23-25), especially at high blowing ratio M=1.2 (Fig.25), the length of the injection flow trace near the leading edge suction side becomes shorter continuously with the incidence angle changing from i=-10 deg (Fig.25(a)) to i=+10 deg (Fig.25(c)). This indicates that the longfillet has effectively eliminated the horseshoe vortex suction side leg in this region that the change of the stagnation point could not affect the vortex flow near leading edge suction side.

The laterally averaged film cooling effectiveness is computed in the region near leading edge suction side. The boundary line of the computing area is the boundaries of narrow region rather than the suction or pressure side. The laterally averaged film cooling effectiveness distribution along the axial chord under different blowing ratio is shown in Fig.12, Fig.17, Fig.22 and Fig.27. When the blowing ratio is M=0.4 (Fig.12(a), Fig.17(a), Fig.22(a), Fig.27(a)), the highest film cooling effectiveness occur at the incidence angle of i=+10 deg for all the geometries, then the film cooling effectiveness decrease as the incidence angle changing from i=+10 deg to i=-10 deg. When the blowing ratio is M=0.8 (Fig.12(b), Fig.17(b), Fig.22(b), Fig.27(b)), the incidence angle of i=0 deg provides the best environment for film cooling near leading edge suction side. When the blowing ratio increases to M=1.2(Fig.12(c), Fig.17(c), Fig.22(c), Fig.27(c)), the trend becomes opposite compared with that of low blowing ratio condition. Especially for longfillet case, the film cooling effectiveness decreases continuously as the incidence angle changing from i=-10 deg to i=+10 deg.

Fig.8, Fig.13, Fig.18 and Fig.23 show the film cooling effectiveness distribution on the entire endwall at different incidence angle, and the blowing ratio is fixed to M=0.4. With the incidence angle changing from i=-10 deg to i=+10 deg, the uncooled area becomes larger especially near the pressure side in the nofillet case. The injection flow traces of the first row of holes are apparently changed by the inlet flow, while the injection flow of following rows in the passage is slightly affected by the inlet flow angle. In the other leading edge geometry cases, the general trend that the uncooled area is larger at positive incidence angle does not change. As the blowing ratio increasing, the effect of incidence angle on endwall film cooling is weakening. Fig.10, Fig.15, Fig.20 and Fig.25 show the film cooling effectiveness distribution on the entire endwall at high blowing ratio of M=1.2. Also only the nofillet case is presented. The effect of the incidence angle could be identified by the injection flow traces exiting from first row of holes. The main part of the endwall platform is protected by the coolant well and no apparent uncooled area could be found, even near the pressure side. Fig.28-31 show the laterally averaged film cooling effectiveness obtained at three incidence angles along the axial chord at specific blowing ratio, in nofillet (Fig.28, Fig.29) and longfillet (Fig.30, Fig.31) cases. For all the four geometry cases the trends in the plots are similar, so only the baseline case and the longfillet case are listed as typical cases. In general, under low blowing ratio the average effectiveness decreases slightly with increasing axial chord distance, while under high blowing ratio the average effectiveness increases with increasing axial chord. As for the low blowing ratio M=0.4 (Fig.28, Fig.30), the effect of incidence angle on the film cooling effectiveness could be identified apparently that with the incidence angle changing form i=-10 deg to i=+10 deg the averaged film cooling effectiveness decreases, while this trend is not obvious at high blowing ratio M=1.2 (Fig.29, Fig.31).

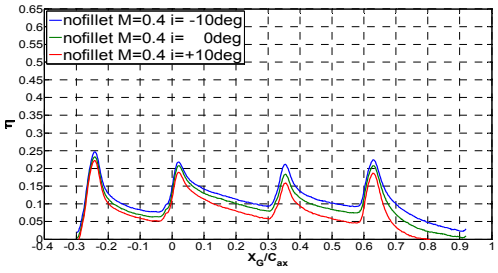

Figure 28. AVERAGED FILM COOLING EFFECTIVENESS.

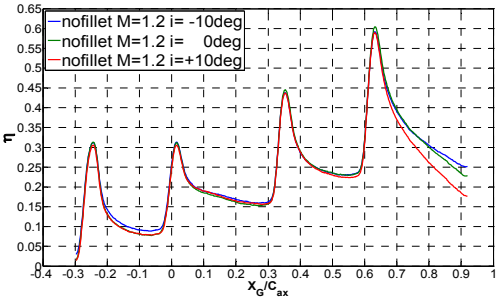

Figure 29. AVERAGED FILM COOLING EFFECTIVENESS.

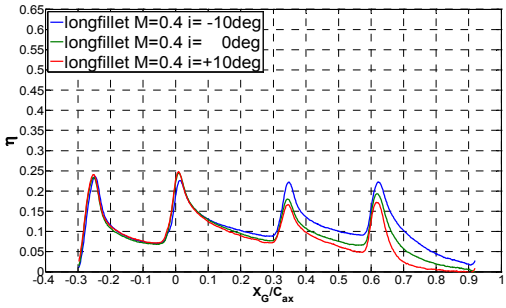

Figure 30.AVERAGED FILM COOLING EFFECTIVENESS.

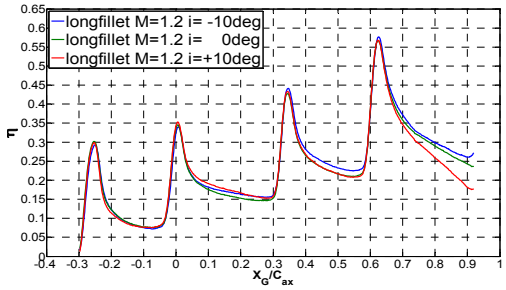

Figure 31. AVERAGED FILM COOLING EFFECTIVENESS.

CONCLUSIONS

An experimental study has been performed to investigate the incidence angle effect on film cooling on endwall with and without fillets. Film-cooling effectiveness has been measured for the endwall surface with and without leading edge fillets at three incidence angles using pressure sensitive paint. Three kinds of fillets with different axial length, as well as the baseline blade were used in the experiment. The effectiveness distribution was presented for leading edge suction side, pressure side and the main passage endwall. In general, the incidence angle affects the coolant jet direction on the leading edge suction side and pressure side. As the incidence angle varies from i=+10 deg to i=−10 deg, at low blowing ratio the film cooling effectiveness decreases near the leading edge suction side for all the leading edge geometries while this trend was turned to be opposite under high blowing ratio that

the lowest film cooling effectiveness condition occurred at the incidence angle of i=+10 deg. Near the leading edge pressure side, the film cooling effectiveness increased as the incidence angle varies from i=+10 deg to i=−10 deg at all blowing ratios in the research and the change of incidence angle cause the peak of laterally averaged effectiveness in this region to shift upstream. The experimental results also indicate that the longfillet has the lowest sensitivity towards incidence angle. As for the main passage endwall platform, with the incidence angle changing form i=-10 deg to i=+10 deg the averaged film cooling effectiveness increases, while this trend will be eliminated by increasing blowing ratio.

ACKNOWLEDGMENTS

The work was partly supported by the National Natural Science Foundation of China (Grant No. 50676043) and the Special Funds for Major State Basic Research Projects (Grant No. 2007CB210108).

NOMENCLATURE

C	=actual chord length of scaled up blade profile
C_{ax}	=axial chord length of the scaled up blade profile
D	=film hole diameter, mm
i	=incidence angle
I	=light intensity
L	=length of film hole, mm
LE	=leading edge
M	=blowing ratio, ρcVc/ρ∞V∞
Ma	=Mach number
P	=blade pitch
PS	=pressure side
PSP	=pressure sensitive paint
Re_{in}	=Reynolds number
S	=span of the scaled up two-dimensional blade
SS	=suction side
V	=velocity, m/s
X, Z	=Cartesian coordinate system
η	=film cooling effectiveness

Subscripts

aw	=adiabatic
c	=Coolant fluid
G	=global coordinate
mix	=mixture condition
ref	=Reference value
∞	=free stream condition

REFERENCES

[1] Yang, H., Gao, Z., Chen, H.C., Han, J.C., and Schobeir, M.T., 2009. "Prediction of Film Cooling and Heat Transfer on a Rotating Blade Platform With Stator-Rotor Purge and Discrete Film-Hole Flows in a 1-1/2 Turbine Stage". *Journal of Turbomachinery*, **131**, pp. 041003/1-12.

[2] Wright, L.M., Blake, S., and Han, J.C., 2006. "Effectiveness Distributions on Turbine Blade Cascade Platforms through Simulated Stator-Rotor Seals". In 9th AIAA/ASME Joint Thermophysics and Heat Transfer Conference, San Francisco, AIAA Paper No.2006-3402.

[3] Gao, Z., Narzary, D., Han, J.C., 2009. "Turbine Blade Platform Film Cooling with Typical Stator-Rotor Purge Flow and Discrete-Hole Film Cooling". *Journal of Turbomachinery*, **131**, pp.041004/1-11.

[4] Charbonnier, D., Ott, P., Jonsson, M., Cottier, F., and Köbke, Th., 2009. "Experimental and Numerical Study of the Thermal Performance of a Film Cooled Turbine Platform". In ASME Turbo Expo 2009: Power for Land, Sea, and Air, Orlando, ASME Paper No.GT2009-60306.

[5] Zhang, L., Moon, H.K., 2003. "Turbine Nozzle Endwall Inlet Film Cooling: The Effect of a Back-Facing Step". In ASME Turbo Expo 2003, collocated with the 2003 International Joint Power Generation Conference, Atlanta, ASME Paper No.GT2003-38319.

[6] Saha, A.K., Mahmood, G.I., and Acharya, S., 2006. "The Role of Leading-Edge Contouring on End-Wall Flow and Heat Transfer: Computations and Experiments". In ASME Turbo Expo 2006: Power for Land, Sea, and Air, Barcelona, ASME Paper No.GT2006-91318.

[7] Mahmood, G.I., Acharya, S., 2007. "Measured Endwall Flow and Passage Heat Transfer in a Linear Blade Passage With Endwall and Leading Edge Modifications". In ASME Turbo Expo 2007: Power for Land, Sea, and Air, Montreal, ASME Paper No.GT2007-28179.

[8] Barberis, D., Molton, P., and Malaterre, T., 1998. "Control of 3D Turbulent Boundary Layer Separation Caused by a Wing–body Junction". *Experimental Thermal and Fluid Science*, **16**, pp.54-63.

[9] Paik, J., Escauriaza, C., and Sotiropoulos, F., 2007. "On the Bimodal Dynamics of the Turbulent Horseshoe Vortex System in a Wing-body Junction". *Physics of Fluids*, **19**, pp.045107/1-20.

[10] Gregory-Smith, D., Bagshaw, D., Ingram, G., and Stokes, M., 2008. "Using Profiled Endwalls, Blade Lean and Leading Edge Extensions to Minimize Secondary Flow". In ASME Turbo Expo 2008: Power for Land, Sea, and Air, Berlin, ASME Paper No.GT2008-50811.

[11] Green, B.E., Whitesides, J.L., 2003. "Method for Designing Leading-edge Fillets to Eliminate Flow Separation". *Journal of Aircraft*, **40**, pp.282-289.

[12] Davenport, W., DeWitz, M., Agarwal, N., Simpson, R., and Poddar, K., 1989. "Effects of a Fillet on the Flow Past a Wing Body Junction". In 2nd Shear Flow Conference, Tempe, AIAA Paper No.AIAA-89-0986.

[13] Kubendran, L.R., Harvey, W.d., 1985. "Juncture Flow Control Using Leading-Edge Fillets". In 3rd Applied Aerodynamics Conference, Colorado Springs, AIAA Paper No.AIAA-85-4097.

[14] Devenport, W.J., Simpson, R.L., Dewitz, M.B., and Agarwal, N.K., 1992. "Effects of a Leading-edge Fillet on the Flow Past an Appendage-body Junction". *AIAA Journal*, **30**, pp.2177-2183.

[15] Gao, Z., Narzary, D., Mhetras, S. and Han, J.C., 2009. "Effect of Inlet Flow Angle on Gas Turbine Blade Tip Film Cooling". *Journal of Turbomachinery*, **131**, pp.031005/1-12.

[16] Montomoli, F., Massini, M., Adami, P., and Martelli, F., 2010. "Effect of Incidence Angle with Wake Passing on a Film Cooled Leading Edge: A Numerical Study". *International Journal for Numerical Methods in Fluids*, **63**, pp.1359-1374.

[17] Lee, S.W., Park, J.J., 2009. "Effects of Incidence Angle on Endwall Convective Transport Within a High-turning Turbine Rotor Passage". *International Journal of Heat and Mass Transfer*, **52**, pp.5922-5931.

[18] Benabed, M., Azzi, A. and Jubran, B.A., 2010. "Numerical Investigation of the Influence of Incidence Angle on Asymmetrical Turbine Blade Model Showerhead Film Cooling Effectiveness". *Heat and Mass Transfer*, **46**, pp.811–819.

[19] Duikeren, B.V., Heselhaus, A., 2008. "Investigations at the Over-Tip Casing of a High Pressure Turbine Including Off-Design Conditions and Heat Transfer Correlations". In ASME Turbo Expo 2008: Power for Land, Sea, and Air, Berlin, ASME Paper No.GT2008-50625.

[20] Wagner, G., Ott, P., Vogel, G., and Naik, S., 2007. "Leading Edge Film Cooling and the Influence of Shaped Holes at Design and Off-Design Conditions". In ASME Turbo Expo 2007: Power for Land, Sea, and Air, Montreal, ASME Paper No.GT2007-2771.